A Finite Elements Approach To The Behaviour of Reinforced Concrete Beam-Column Joints

K. F. Sarsam
University of Technology, Building & Construction Department, Head of Structural Branch.
A. N. Attiyah
Kufa University, College of Engineering, Head of Civil Department
M. A. Attiyah
Ass. Lec., Kufa University, College of Engineering, Civil Department

Abstract

This paper describes a three-dimensional nonlinear finite element techniques used to successfully model reinforced concrete beam-column joint specimens subjected to non-proportional axial and shear loads. A 20-noded isoparametric brick element had been used to model the concrete. The reinforcing steel bars were idealized as axial members embedded within the brick elements. Perfect bond between the concrete and the reinforcing bars was assumed. The behaviour of concrete in compression was simulated by an elasto-plastic work hardening model followed by a perfect plastic response, which was terminated at the onset of crushing. In tension, a fixed smeared crack model had been used with a tension-stiffening model to represent the retained post-cracking tensile stresses and a shear retention model that modified the shear modulus after cracking. The nonlinear equations of equilibrium have been solved using an incremental-iterative technique operating under load control. The solution algorithms used were the standard and modified Newton-Raphson method. The numerical integration has been conducted using the 27-point Gaussian type rule. Two types of reinforced concrete beam-column joints had been analyzed and the finite element solutions were compared with the experimental data. Several parametric studies have been carried out to investigate the effect of some important finite element and material parameters on the predicted finite element results. The study included the effect of concrete compressive strength, column axial load, beam tension and compression reinforcement, and beam shear span to depth ratio.

الخلاصة

استخدم في هذه الدراسة نموذجاً لا خطياً ثلاثي الأبعاد للعناصر المحددة ملائم لتحليل المفاصل بين العتبات والأعمدة "Beam-column joints" تحت تأثير حمل غير متناسق "Non-proportional loading" . استخدم العنصر الطابوقي ذو العشرين عقدة لتمثيل الخرسانة أما حديد التسليح فقد مثل بعناصر محورية مطمورة داخل العناصر الطابوقية . أعتبر تصرف الخرسانة في الانضغاط تصرفاً مرناً – لدناً يتبعه تصرفاً لدناً تاماً ينتهي عند تهشم الخرسانة. أما سلوك الخرسانة تحت تأثير إجهادات الشد فقد اعتمد نموذج الشق المنتشر "Smeared crack model" لتمثيله وأدخل نموذج تصلب الشد "Tension-stiffening model" . وقد تبني نموذج احتباس القص "Shear-retention model" والذي يقوم بتخفيض قيمة معامل الصلابة المتبقي مع استمرار التحميل في مرحلة ما بعد التشقق . تم حل معادلات التوازن اللاخطية باستخدام تقنية تزايدية – تكرارية "Incremental-iterative technique" تعمل تحت أحمال مسيطرة . أجريت التكاملات العددية باستخدام قواعد التكامل ذات 27 نقطة تكامل . تم تحليل نوعين من المفاصل بين العتبات والاعمدة الخرسانية المسلحة وقورنت النتائج المستحصلة من طريقة العناصر المحددة مع النتائج العملية . تم دراسة العديد من المتغيرات لمعرفة تأثيرها منها مقاومة الانضغاط للخرسانة وحمل العمود المحوري و التسليح الطولي لحديد الشد والضغط في العتبات ونسبة طول العتبة إلى عمقها.

1. Introduction

In general, analysis and design of buildings, the structures that contain slabs, beams, and columns are referred to as "RIGID FRAMES". However, research indicates that, both in reinforced concrete and structural steel frames, the beam-column joint is definitely not rigid; it is subjected to deformation under all type and stages of loading. In addition, extensive research shows that failure may occur at the joint instead of at the column or the beam. Thus, another way of looking at a joint is to consider it as a member of the structure, as is the case for slabs, beams, columns, … etc. A joint is defined as that portion of the column within the depth of the beam(s) that frame into column(ACI-ASCE,1985**)**. ACI-ASCE committee **352** divided the monolithic reinforced concrete beam-column joints into two types:

Type 1 Joint: It is a joint in a continuous moment resisting structure designed on the basis of strength without considering special ductility requirements.

Type 2 Joint: It is a joint that connects members, which are required to dissipate energy through reversals of deformation into the inelastic range.

At present, with the development of digital computers and numerical techniques, the finite element method has emerged as a powerful tool for engineers to model rationally many aspects of the phenomenological behavior encountered in concrete. These aspects include the non-linear multiaxial properties, modeling of cracking and crushing of concrete, the changes in material properties after cracking of concrete and yielding of reinforcing steel, and many other properties.

2. Finite Element Formulation And Nonlinear Solution Techniques

2.1 Material Representation

Concrete Idealization: The 20-noded isoparametric element is used for this work, and it is shown in Fig. (1).

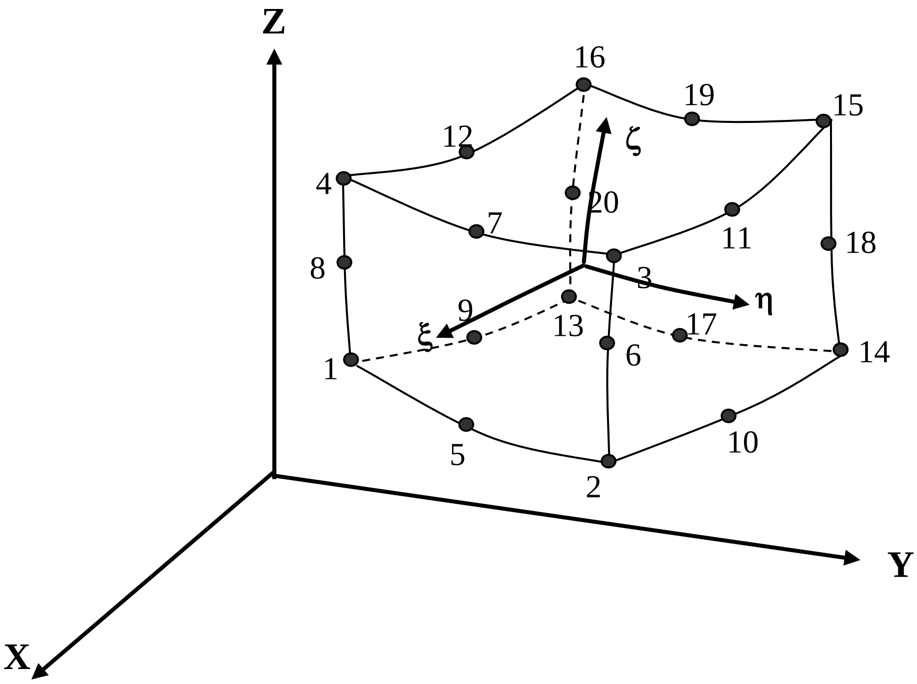

Figure (1): The 20-noded brick element in Cartesian coordinates

The natural local coordinate system (Robinson,1973) (ξ,η,ζ) is used to express the displacement components. The origin of the local coordinate system is the center of the element as shown in Fig. (1). The element sides are defined in the local coordinate system by:

$\xi = \pm 1$, $\eta = \pm 1$, $\zeta = \pm 1$.

Reinforcement Representation: this study adopts the embedded representation shown in Fig. (2), which is almost used in connection with the higher order isoprametric concrete elements. The reinforcing bar is considered to be an axial member built into the isoprametric concrete element such that its displacements are consistent with those of the element. Perfect bond is assumed between concrete and reinforcing steel bars.

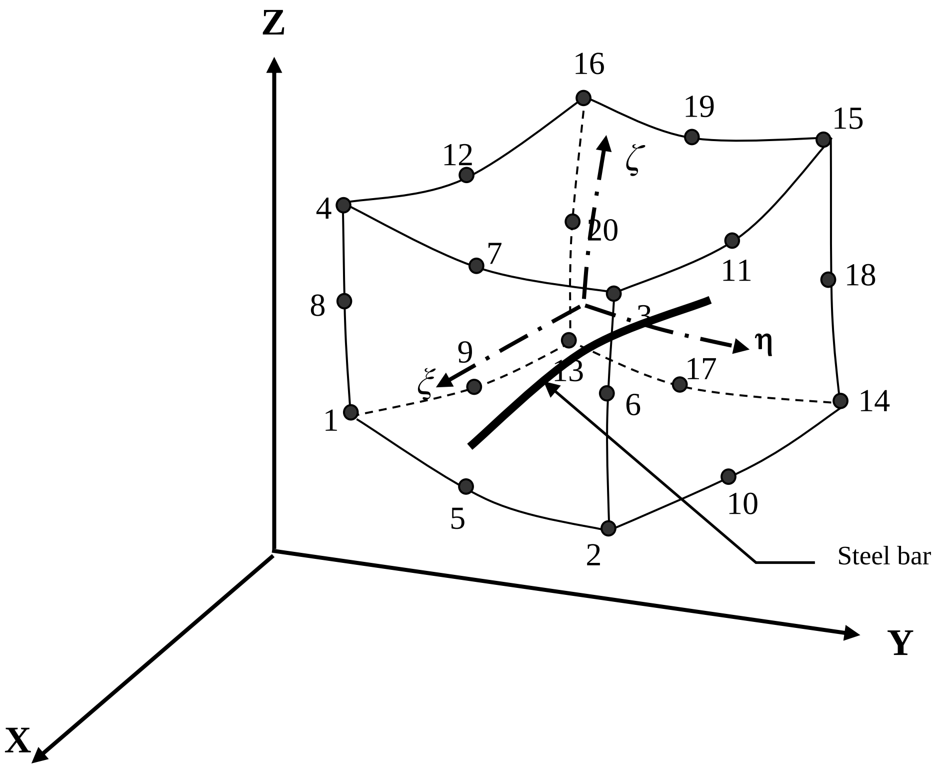

Figure (2): Representation of embedded reinforcement.

2.2 Numerical Integration

The evaluation of the stiffness matrices and the equivalent nodal loads involves integration. Explicit integration for these functions may be very difficult or, even impossible. Therefore, an alternative arrangement of numerical integration is usually used. The 27(3×3×3) Gauss-quadratic integration rule has been used in this investigation. The relative position of the sampling points for this rule over the volume of the brick element is shown in Fig. (3).

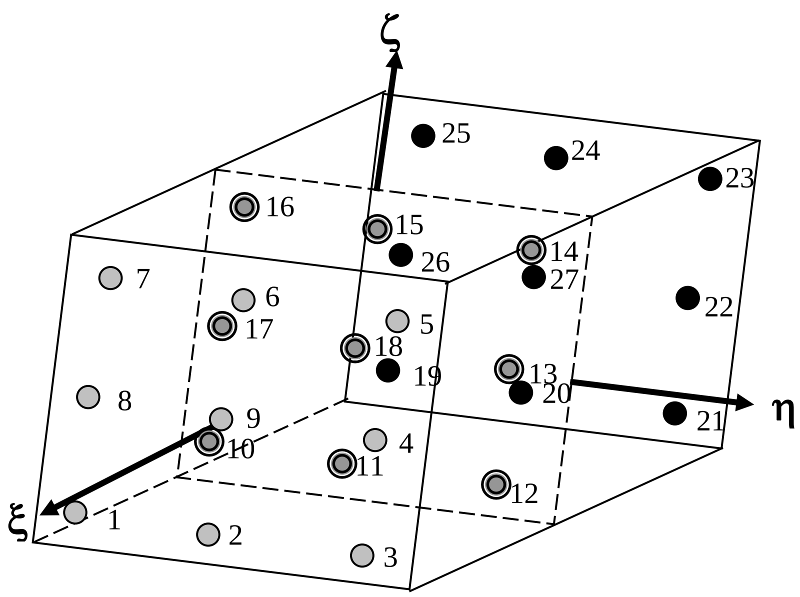

Figure (3): Distribution of the sampling points over the element (27-points integration rule).

2.3 Nonlinear Solution Techniques

The Incremental-Iterative method is the most commonly used technique for solving non-linear finite element problems. It implies the subdivision of the total external load into smaller increments; within each increment of loading iterative cycles are performed in order to obtain a converged solution corresponding to the stage of loading under consideration,see Fig. (4).

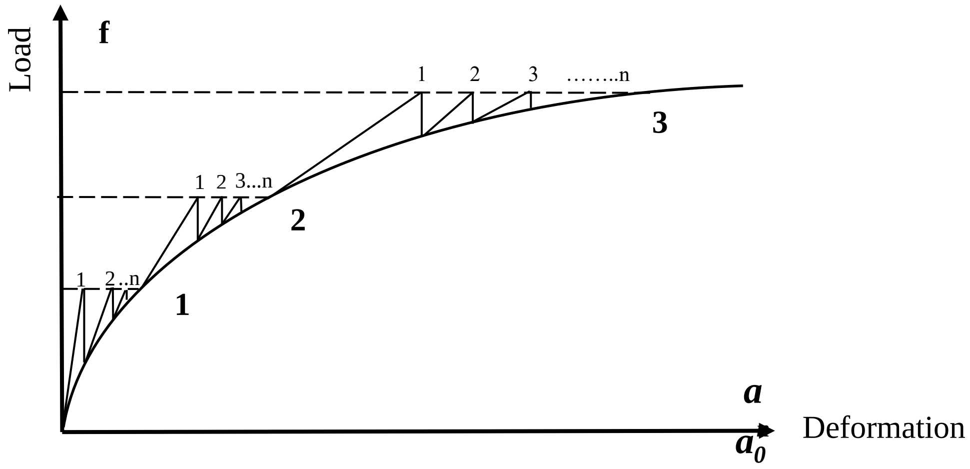

Figure (4): Incremental- iterative techniques

2.4 Convergence Criteria

The force convergence criterion has been considered in the numerical analyses carried out in the present work. When the residual (out of balance) forces are sufficiently small, the convergence is assumed to occur. Hence this criterion can be expressed in the form:

$$\frac{\|\{x\}\|}{\|\{y\}\|} * 100\% \leq TOL \qquad (1)$$

Where: $\|\{x\}\| = \sqrt{(\{x\}^T\{x\})}$

$\|\{y\}\| = \sqrt{(\{y\}^T\{y\})}$

3. Numerical Modeling of Concrete Properties

3.1 Behaviour of Concrete in Compression

The accuracy of the numerical material model that may be adopted in the analysis should trace the overall behaviour of the member within sufficient degree of accuracy. In the present study, the behaviour of concrete in compression is simulated by an elasto-plastic work hardening model followed by perfect plastic plateau, which is terminated at the onset of crushing.

The incremental theory of plasticity is based on following fundamental assumptions: yield criterion, hardening rule, flow rule and crushing condition.

The Yield Criterion: under multidimensional states of stress, the yield criterion for concrete is generally assumed to be dependent on three stress invariants However, many studies assumed that a yield criterion can be adequately expressed in terms of two-stress invariants only (I_1 and J_2) as

$$f(\{\sigma\}) = f(I_1, J_2) = (\alpha I_1 + 3\beta J_2)^{1/2} = \sigma_0 \qquad (2)$$

where

α and β are material parameters.

I_1 and J_2 are the first stress invariants and the second deviatoric invariant, respectively that are given by:

$$I_1 = \sigma_x + \sigma_y + \sigma_z \tag{3}$$

$$J_2 = \frac{1}{3}[(\sigma_x{}^2 + \sigma_y{}^2 + \sigma_z{}^2) - (\sigma_x.\sigma_y + \sigma_y.\sigma_z + \sigma_x.\sigma_z)] + \tau_{xy}{}^2 + \tau_{yz}{}^2 + \tau_{zx}{}^2 \tag{4}$$

The stress σ_o is the equivalent effective stress at the onset of plastic deformation that can be determined from uniaxial compression test as:

$$\sigma_o = C_p . f_c' \tag{5}$$

where: *Cp*. is plasticity coefficient used to mark the initiation of plastic deformation,so $0 < Cp < 1.0$

The Hardening Rule: The hardening rule is required to define the change of position of the loading surfaces during plastic deformation. A relationship between the accumulated plastic strain and the effective stress is required to control the position of the current loading surface. A number of hardening rules have been proposed to describe the growth of the subsequent loading surfaces for a work hardening material. In the present study an isotropic hardening rule is adopted (Ohtani, and Chen,1988) . Therefore, Eq. (2) can be expressed for the subsequent loading functions as:

$$f(\sigma) = C.I_1 + \{(C.I_1)^2 + 3\beta J_2\}^{1/2} = \sigma' \tag{6}$$

where: σ' represents the stress level at which further plastic deformation will occur. The effective stress-plastic strain relationship can be expressed as:

$$\sigma' = C_p . f_c' - E\varepsilon_p + \left(2E^2 \varepsilon_o' \varepsilon_p\right)^{1/2} \tag{7}$$

where: ε_o' is total strain

The uniaxial stress-strain curve is assumed to be linear up to stress level equal to $Cp.f_c'$ followed by a parabolic shape up to the peak compressive stress f_c'. In the current study, values of 03 05 are assumed for plastic coefficient *Cp* for normal and high strength concrete respectively. The plastic yielding begins at a stress level of $Cp.f_c'$. If Cp=1.0, then the elastic perfectly plastic behaviour is specified, as shown in Fig. (5).

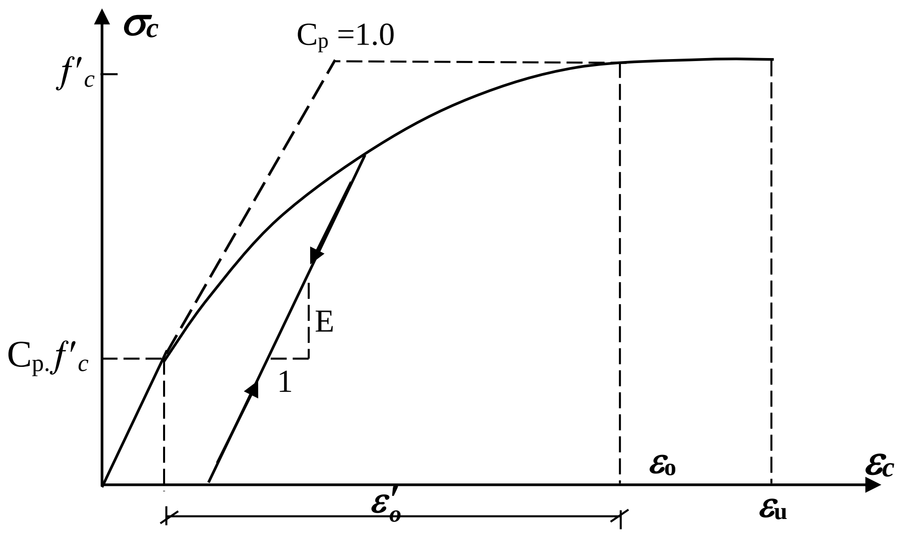

Figure (5): Uniaxial stress-strain curve of concrete in compression

In order to connect the loading function ***f*** and the stress-strain relation in the plastic range, an associated flow rule is usually employed. This means that the plastic deformation rate vector will be assumed to be normal to yield surface. The plastic strain increment is defined as:

$$d\{\varepsilon_p\} = d\lambda \frac{\partial f(\{\sigma\})}{\partial\{\sigma\}} \tag{8}$$

The normal to the current loading surface is termed as the flow vector. The yield function derivatives with respect to the stress components define the flow vector *{a}* as*:*

$$\{a\}^T = \left\{ \frac{\partial f}{\partial \sigma_x}, \frac{\partial f}{\partial \sigma_y}, \frac{\partial f}{\partial \sigma_z}, \frac{\partial f}{\partial \tau_{xy}}, \frac{\partial f}{\partial \tau_{yz}}, \frac{\partial f}{\partial \tau_{zx}} \right\} \tag{9}$$

The Crushing Condition: In the adopted model, the isotropic expansion of the subsequent loading surface is terminated when the effective stress reaches the peak compressive stress. Beyond that a perfectly plastic response is assumed to occur. Perfectly plastic flow continues until the ultimate deformation capacity of concrete is reached and the material eventually exhibits a crushing failure. The stresses at the crushed point drop abruptly to zero. The crushing criterion is obtained by simply converting in Eq. (2), which is in terms of stresses directly into strain (Chen,1982), thus:

$$cI_1' + \left\{ (cI_1')^2 + 3\beta J_2' \right\}^{1/2} = \varepsilon_{cu} \tag{10}$$

where: ε_{cu} is the ultimate strain value which can be extrapolated from the uniaxial compression test.

I_1' and J_2' are the first strain invariant and the second deviatoric strain invariant respectively.

3.2 Behaviour of Concrete in Tension

The cracking criterion: In the present study, the initiation of cracking is controlled by a maximum tensile stress criterion. At the sampling point under consideration, if the major principal stress,σ, exceeds the limiting tensile strength a crack is assumed to form. The limiting tensile stress required to define the onset of cracking can be calculated for the state of triaxial tensile stress and for combinations of tension and compression principal stresses as follows (Zienkieweicz et al.,1972 and Bathe and Sundberg, 1986) :

a) For the triaxial tension zone: ($\sigma_1 \geq \sigma_2 \geq \sigma_3 > 0$)

$$\sigma_i = \sigma_{cri} = f_t \qquad i = 1,2,3,.... \tag{11}$$

b) For the case of the tension-tension-compression zone:

($\sigma_1 \geq \sigma_2 > 0, \sigma_3 \leq 0$)

$$\sigma_i = \sigma_{cri} = f_t \left[1.0 + \frac{0.75\sigma_3}{f_c'} \right] \qquad i = 1,2,3,.... \tag{12}$$

c) For the case of tension-compression-compression zone:

($\sigma_1 > 0$, $\sigma_2 \leq \sigma_3 \leq 0$)

$$\sigma_i = \sigma_{cri} = f_t \left[1.0 + \frac{0.75\sigma_2}{f_c'} \right] . \left[1.0 + \frac{0.75\sigma_3}{f_c'} \right] \tag{13}$$

where: σ_{cr} is the cracking stress and f_t, f_c' are the tensile and compressive concrete strength (positive value).

Tension-Stiffening Model: Tension-stiffening effect is found to be quite significant under service load conditions by increasing the overall strength of the system in the post cracking range.

In finite element modeling of reinforced concrete two approaches have been suggested to account for these effects, the first approach is characterized by increasing the stiffness of steel bars. The second approach is characterized by a gradual decrease of the tensile stress in the cracked concrete cover a specified strain range. Many researchers used the second approach to account for the tension-stiffening effect as shown in Fig.(6) conventionally reinforced concrete members.

In a current work, the second approach is adopted to represent the tension-stiffening effect.

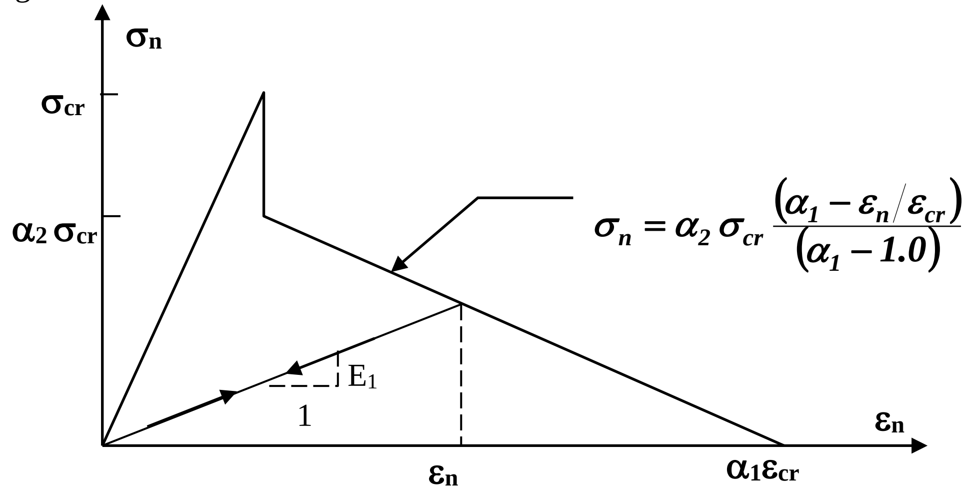

Figure (6): Post-cracking model for concrete in tension

3.3 Behaviour of steel

Steel bar can be assumed to transmit axial force only. Modeling of steel in condition with the finite element analysis of reinforced concrete members is much simpler than the modeling of concrete.

In the present study, the uniaxial stress-strain behaviour of reinforcement is simulated by elastic linear work hardening model (Al- Shaarbaf,1990) , as shown in Fig. (7).

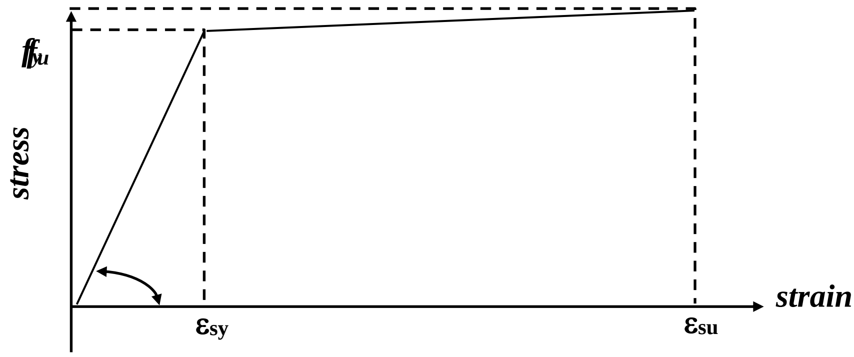

Figure (7): Stress-strain relationship of steel bars used in the analysis

4. Numerical Examples

To demonstrate the applicability of the method developed in the present study two types of reinforced concrete joints have been analyzed to investigate the behaviour of joints under monotonic loads using the nonlinear finite element analysis. A mathematical model suitable for the nonlinear analysis of reinforced concrete joints under monotonically increasing load has been developed in the present research work. The accuracy and efficiency of the proposed model were examined by comparing the analytical finite element results with the experimental results. Also, the effects of some numerical and material parameters on the prediction of the overall behaviour of joints have been studied. The effect of concrete compressive strength, effect of tension reinforcement ratio, influence of column axial load (Nu), presence of hoops, influence of (a_v/d_b) are also studied.

4.1 Sarsam Reinforced Concrete Beam-Column Joints

Sarsam, in 1983 tested experimentally nine reinforced concrete joints under monotonic loads. The selected joints were designated as EX2 and IN1. The analytical load deflection response of all selected joints was compared with the experimental load-deflection curve.

4.1.1 Loading Procedure of Test Specimens

For exterior specimens (EX) the column was first loaded to a predetermined value (Nu) prior to any beam loading. The column axial load was kept constant during testing of all specimens. At this stage, the initial zero reading of deflection, and concrete surface strains were taken and recorded. The next stage involved loading the beam (V_u). This was done by several stages of loading. During each stage, several straining measurements were taken and deflection values were recorded at the loaded end of beam. The interior specimens (IN1) were tested in the same way as the exterior ones. With controlling column load at an approximately constant amount, the next in specimen (IN1) stage involved beam loading, where the north beam was loaded (V_u) with the south beam acting as a reaction beam (V_R) in the statically indeterminate sub-frame.

4.1.2 Description of Test Specimens

The details of the reinforced concrete beam-column joints, which were adopted in this work, are shown in Figs.(8),(9). The column outside the joint was reinforced with four 16mm longitudinal bars and 8mm closed ties at 85mm c/c spacing. All specimens used in this work, except EX2, had 3-8mm closed hoops in the joint. The part representing the beam was reinforced with two 16mm bars on the tension side and two 12mm bars on the compression side. Beam stirrups were 8mm closed bars at 130mm c/c.

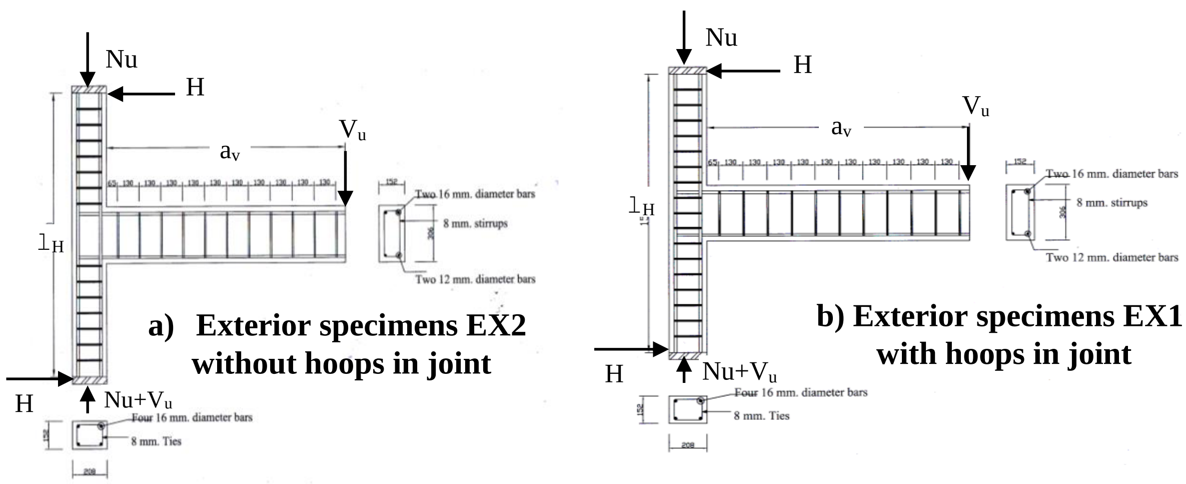

a) Exterior specimens EX2 without hoops in joint

b) Exterior specimens EX1 with hoops in joint

Figure (8): Dimension and reinforcement details of exterior beam-column joints (*all dimensions in mm*)

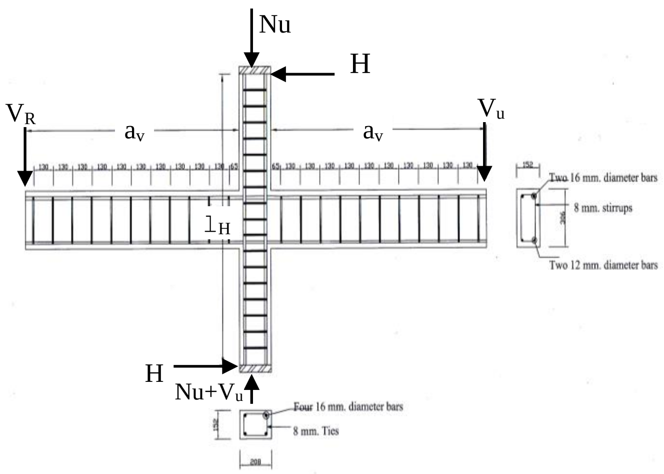

Figure (9): Dimension and reinforcement details of interior beam-column joints
(*all dimensions in mm*)

4.1.3 Finite Element Idealization

By taking into consideration the geometry and loading symmetry. One half of the joint has been considered in this analysis. This half was modeled using the 20-node isoparametric brick element. The selected half of the joints of series EX was discretized into (12) elements, while for the joints of series IN, the selected half was discretized into (18) elements. The finite element meshes, boundary conditions and loading arrangement for series EX and IN are shown in Figs. (10) and (11). The material properties and the additional material parameters adopted in the finite element analyses are listed in table (1).

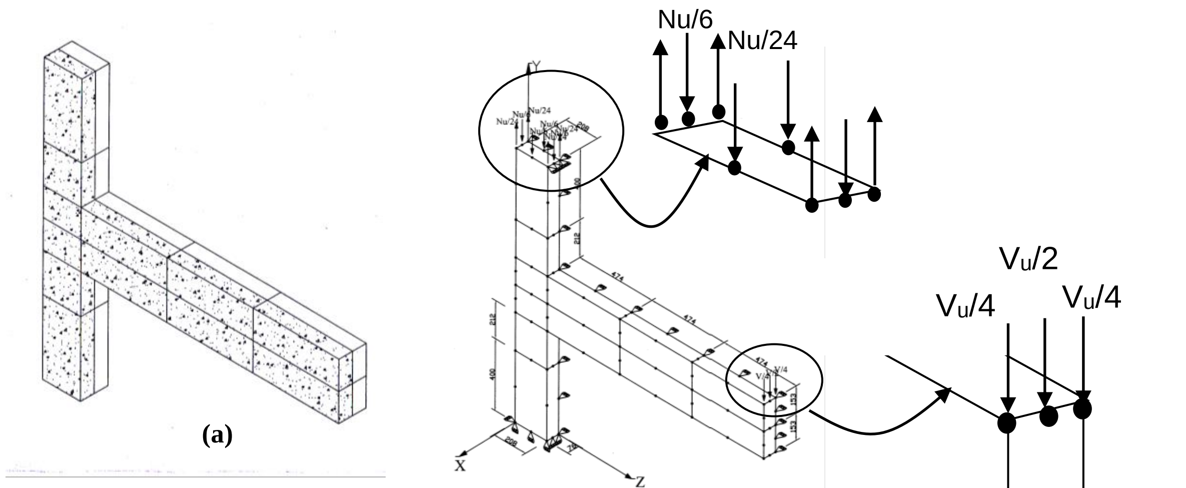

(a)

(b) Equivalent nodal forces used in the present study

Figure (10): Finite element idealization, boundary and symmetry condition for exterior joint with (12) elements.

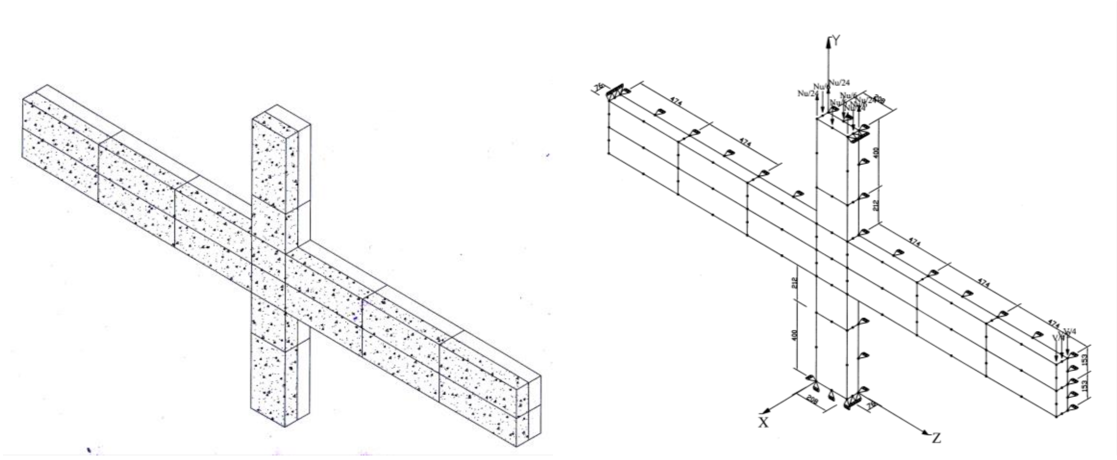

Figure (11): Finite element idealization, boundary and symmetry condition for interior joint with (18) elements.

Table (1): Dimensions, material properties and additional parameters used for Sarsam's joints

Joint				EX1	EX2	EX3	EX4	IN1
Dimension	*Beam*		av (mm)	1422	1422	661	883	1422
			b_b (mm)	152	152	152	152	152
			h_b (mm)	303	305	30z5	305	305
	Column		ℓ_H (mm)	1531	1536	1532	1537	1530
			b_c (mm)	152	152	152	152	152
			h_c (mm)	205	204	204	204	204
Concrete	Young modulus E_c (MPa)			35.5	33.0	28.0	32.6	32.4
	Compressive strength f'_c(MPa)			56.3	53.9	41.3	49.3	53.6
	Tensile strength f_t (MPa)			4.24	3.38	3.44	3.87	4.31
	Poisson's ratio			0.2	0.2	0.2	0.2	0.2
	Uniaxial crushing strain ε_{cu}			.004	.004	.004	.004	.004
steel	Beam reinforcement	Top bars	Bar diameter (mm)	16	16	16	16	16
			Number of bars	2	2	2	2	2
			Yield Stress. f_y (MPa)	504	504	504	504	504
			Area of steel (mm^2)	199	199	199	199	199
		Bott. bars	Bar diameter (mm)	12	12	12	12	12
			Number of bars	2	2	2	2	2
			Yield Stress. f_y (MPa)	507	507	507	507	507
			Area of steel (mm^2)	113	113	113	113	113
		Stirr. bars	Bar diameter (mm)	8	8	8	8	8
			Distance c/c	130	130	130	130	130
			Yield Stress. f_y (MPa)	517	517	517	517	517
			Area of steel (mm^2)	51.5	51.5	51.5	51.5	51.5
	Column reinforcement	Long. bars	Bar diameter (mm)	16	16	16	16	16
			Number of bars	4	4	4	4	4
			Yield Stress. f_y (MPa)	504	504	504	504	504
			Area of steel (mm^2)	199	199	199	199	199
		Tie bars	Bar diameter (mm)	8	8	8	8	8
			Distance c/c	85	85	85	85	85
			Yield Stress. f_y (MPa)	517	517	517	517	517
			Area of steel (mm^2)	51.5	51.5	51.5	51.5	51.5
	Hardening parameter			0.0	0.0	0.0	0.0	0.0
Numerical parameter	Tension-stiffening Parameter		α_1	60	60	50	50	65
			α_2	0.5	0.4	0.5	0.6	.65
	Shear retention Parameter		γ_1	20	20	20	20	20
			γ_2	0.5	0.5	0.5	0.5	0.5
			γ_3	0.15	0.15	0.15	0.15	0.2
	Compression strength reduction parameter K_1			0.5	0.5	0.5	0.5	0.5

5. Results Of Analysis

This section presents the results obtained from the finite element analysis carried out for the chosen joints.

The experimental and numerical load-tip deflection curves for joints EX2 and IN1 are shown in Figs. (12) and (13). Good agreement was obtained for the finite element solution compared with experimental results. The predicted response is approximately similar to the experimental response throughout the entire range of loading. However, the ultimate load obtained from finite element analysis is slightly higher than the actual experimental ultimate load.

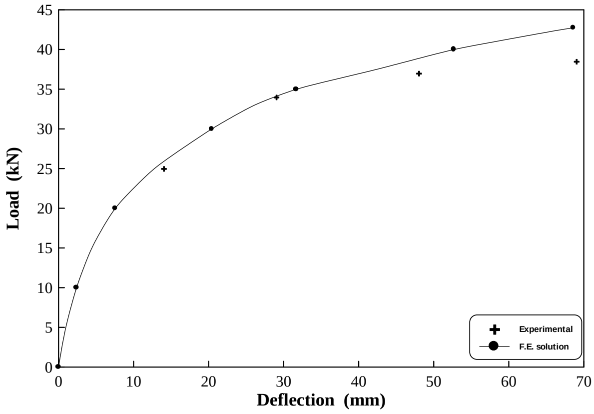

Figure (12): Joint EX2 Load-deflection behaviour.

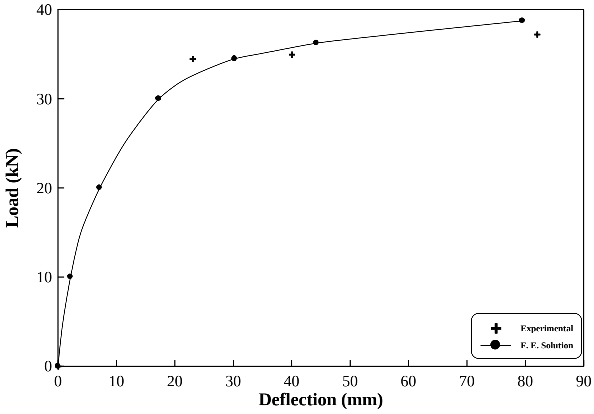

Figure (13): Joint IN1 Load-deflection behaviour.

The predicted ultimate load capacity obtained from the finite element analysis for joints EX2 and IN1 together with the corresponding experimental load are shown in table (2). The table reveals that there is a good agreement between the analytical and the experimental results.

Table (2): Comparison between experimental and predicted collapse load

Joint	V_u exp. (kN)	V_u F.E.Sol. (kN)	V_u F.E.Sol./ V_u exp.
EX2	38.5	42.75	1.11
IN1	37.25	38.75	1.04

5.1 Parametric Study

A purpose of the overall research programs to optimize the design of beam-column joints. The parametric study of the beam-column joint behaviour is necessary for design optimization. joint EX2 were chosen to study the effect of several important parameters behaviour and ultimate moment capacity of beam-column joint.

5.1.1 Influence of Column Axial Load

One of the primary considerations in the design of beam-column joints is the axial load capacity. Transmission of the axial load through the joint region requires adequate lateral confinement of concrete in the column by action of longitudinal column reinforcement plus either transverse members framing into the column or transverse reinforcement.

In order to investigate the effect of the column axial load on the load-deflection behaviour and ultimate load of the beam-column joint, joints EX2 have been tested with axial loads equal to 0, 100, 300, 500, 600kN. Fig. (14) shows that the presence of axial compression loads results in an increase in the shear strength of the joint. The predicted collapse loads were 37.5, 40, 42.75, 44.5 and 45.25kN, for column axial load 0, 100, 300, 500 and 600kN respectively.

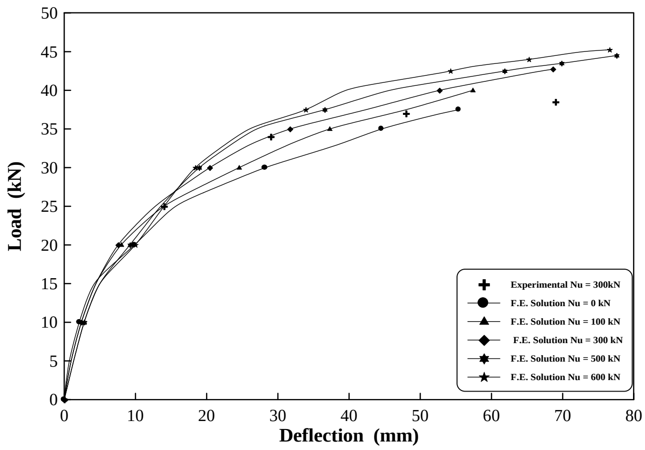

Figure (14): Joint EX2 effect of column axial load on the load-deflection behaviour

5.1.2 Influence of Grade of Concrete

Different concrete strength was used in the model to predict the load-deflection of beam-column joint. The selected values of concrete compressive strength were 30, 40, 60 and 70MPa, in addition to the actual strength of the experimentally tested specimen, which was 54MPa for both joints. Figs. (15) reveal that a response stiffer than the experimental curve is noted for higher grades of concrete and softer response is noted for lower grades of concrete. The predicted collapse loads are listed in table (5.3). Therefore, it can noted that the compressive strength of concrete strongly affects the ultimate shear capacity reinforced concrete beam-column joints.

Table (3): Effect of grade of concrete on the ultimate load capacity

Grade of concrete (MPa)	Collapse load (kN)
	EX2
30	32
40	37
50	42.75
60	47.5
70	54

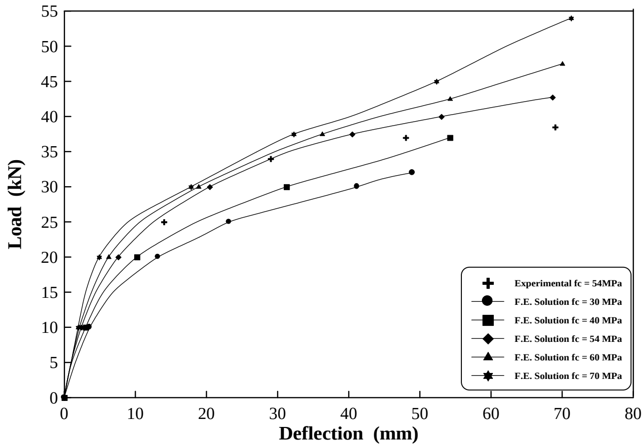

Figure (15): Joint EX2 effect of compressive strength of concrete on the load-deflection behaviour

5.1.3 Influence of Beam Shear Span to Depth Ratio

The effect of beam shear span to depth ratio (a_v/d_b) was investigated in this research work. Joint EX2 with three different (a_v/d_b) ratios which (2.43, 3.22 and 5.26) were used in this analysis. The table (4) shows the predicted ultimate shear strength obtained using these ratios.

Table (4): Effect of beam shear span to depth ratio on the load carrying capacity

Specimen	a_v/d_b	V_u kN
EX2	5.26	47.75
	3.22	68.5
	2.43	81.75

The table reveals that the shear span to depth ratio has a significant effect on the ultimate load capacity of the joint. This may be attributed to the increase in the stress generating at the compression zone of joint due to the increase in the value of moment developed at the face of the column.

5.1.4 Effect of Longitudinal Steel

In the present research work, a study was made to investigate the influence of the amount of tension and compression steel reinforcement used in the beams, on the load-deflection behavior of joints. Joint EX2, which have been used in this analysis. The amount of tension and compression reinforcement used in the finite element analysis was 1, 1.5 and 2 times the amount used in the experimental work.

Fig. (16) reveal that the increase in the area of longitudinal tension steel bars results in a slightly stiffer post cracking response and predicted ultimate load capacity increased. That means, the tension reinforcement steel bars have yielded before the compression reinforcement steel bars. Therefore, a substantial increase in post cracking stiffness and ultimate load capacity was obtained with increasing the amount of tension steel. However the post cracking stiffness and ultimate load capacity are slightly affected by increasing the compression steel bars, Fig. (17). The predicted ultimate load and the ratio of the predicted ultimate load to the value of experimental ultimate are listed in Table (5).

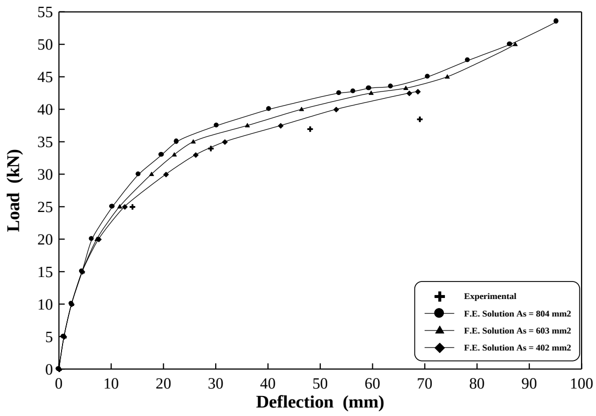

Figure (16): Joint EX2 effect of the variation of steel area of top longitudinal bars, on the load-deflection behaviour.

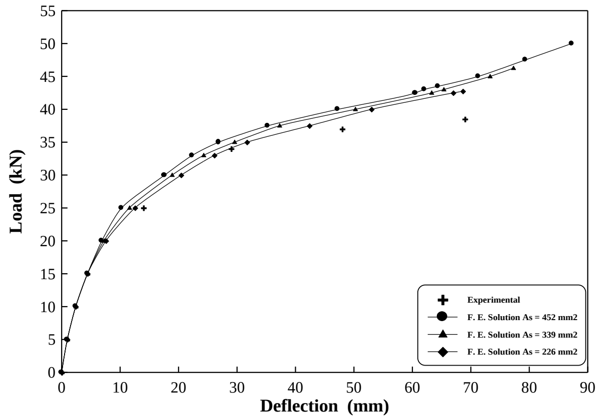

Figure (17): Joint EX2 effect of the variation of steel area of bottom longitudinal bars, on the load-deflection behaviour.

Table (5): Effect of amount longitudinal reinforcement in the load carrying capacity

Specimen		V_u F. E. Solution (kN)	V_u experimental (kN)	$\frac{V_u \text{ F.E. S.}}{V_u \text{ exp.}}$	$\frac{\text{As F.E.S.}}{\text{As exp.}}$
EX2	Tens. steel	42.75	38.5	1.11	1
		50		1.3	1.5
		54.5		1.42	2
	Comp. steel	42.75	38.5	1.11	1
		46.25		1.2	1.5
		50.5		1.312	2

6. Conclusions

1. The three-dimensional nonlinear finite element model, which was adopted in the present work, is suitable for predicting the behaviour of the reinforced concrete joints subjected to non-proportional monotonically increasing loading. The numerical results were in good agreement with experimental load-deflection results throughout the entire range of behaviour.
2. The results indicate that the value of column axial load has significant effect on the response of joints. The shear strength of the joint increased as the value of column axial load increased.
3. The predicted ultimate load carrying capacity of joints was found to depend on the grade of concrete. The results revealed that an increase of (70)% in the ultimate load when a compressive strength of concrete for specimen EX2 increased from 30 MPa to 70 MPa.
4. The results indicate that the increase in the area of longitudinal tension steel bars had a significant effect on post-cracking response and predicted ultimate

load value increased. However, the post cracking stiffness and ultimate load capacity were only slightly affected by increasing the compression steel bars.

7. References

ACI-ASCE committee 352 Report, "Recommendations for Design of Beam-Column Joints in Monolithic Reinforced Concrete Structure", ACI Journal, Vol. 82, No. 3, May-June, 1985, PP. 266-283.

Al- Shaarbaf I.A.S, "Three-Dimensional Nonlinear Finite Element Analysis of Reinforced Concrete Beams in Torsion" Ph.D. Thesis, University of Bradford, 1990, 323 pp..

Bathe, K.J., and Sundberg, J.A., "A concrete Material Model", In the Computational Modeling of Reinforced Concrete Structure, Edited by Hinton, E., and Owen., R., Pineridge Press, Swansea, 1986, pp.101-121.

Chen, W. F., "Plasticity on Reinforced Concrete", McGraw-Hill Book Company, 1982, 474 PP.

Ohtani, Y., and Chen, W., F., "Multiple Hardening Plasticity for Concrete Materials", Journal of Engineering Mechanics, Vol. 114, No. 11, November 1988.

Robinson, J., "Integrated Theory of Finite Element Methods", John Wily and Sons, England, 1973, 428 PP.

Sarsam, K. F., "Strength and Deformation of Structural Concrete Joints", Ph.D. Thesis, University of Manchester, 1983, 340 pp.

Zienkieweicz, O.C., Owen, D. R. J., Phillips, D.V., and Nayak, G.C., "Finite Element Methods in the Analysis of Reactor Vessels", Nuclear Engineering and Design, Vol. 20, No. 2, 1972, PP.507-541.